

Synthesis of Activated Carbon from a Bio Waste (Flower of Shorea Robusta) Using Different Activating Agents and Its Application as Supercapacitor Electrode

Souvik Ghosh^{***}, Prakas Samanta^{***}, Naresh Chandra Murmu^{***},
Nam Hoon Kim^{***†}, Tapas Kuila^{***†}

ABSTRACT: The activated carbon is a very good choice for using as supercapacitor electrode materials. Herein, the flower of Shorea robusta, a bio-waste material was successfully used to synthesize the activated carbons for application as supercapacitor electrode materials. The activated carbon was synthesized through chemical activation process followed by thermal treatment at 700°C in presence of N₂ atmosphere using KOH, ZnCl₂ and H₃PO₄ as the activating agents. The physicochemical analyses demonstrate that the obtained activated carbons are graphitic in nature and the degree of disorder of the graphitic carbons is changed with the activating agents. The activated carbon obtained from Shorea robusta flower (ACSF-K) electrode shows the specific capacitance of ~610 F g⁻¹ at 2 A g⁻¹ current density, which is higher than ACSF-Z (560 F g⁻¹) and ACSF-H (470 F g⁻¹) electrode material under the identical current density. The synthesized graphitic carbons also demonstrated good rate capability and high electrochemical stability as supercapacitor electrode.

Key Words: Flower of Shorea robusta, Bio-waste materials, Graphitic carbon, Supercapacitor

1. INTRODUCTION

The rapid depletion of fossil fuel and the increase in energy demand have forced the researchers to develop solar and wind energy as sustainable, clean and renewable energy sources [1]. In addition to the development of renewable energy sources, the scientific community also recognizes that the development of inexpensive and efficient energy storage devices such as batteries, fuel cells and supercapacitors should also be promoted [2]. In comparison to the various energy storage devices, supercapacitor is considered as the emerging device for pulse power applications due to its high power density, long life span and wide operating temperature range. Various carbonaceous materials such as, graphene, carbon nanotube, carbon aerogels and activated carbon are used as supercapacitor electrode

material [3]. Among these, activated carbons are one of the most widely used supercapacitor electrode material due to its high active surface area, porous nature, high electrical conductivity and high chemical stability [4]. Recently, synthesis of activated carbon from bio-waste gets considerable attention as supercapacitor electrode materials owing to its easy accessibility, low cost and most importantly non toxicity [5]. The flowers of Sal (Shorea robusta) are generally wasted in every year in forest fringe areas. The holistic flower of Sal has a quarry of bioactive constituents with high amount of carbon sources like alkaloids, carbohydrates, flavonoids, glycosides, etc [6]. The weight of the Sal flower is also very light, indicating a high specific surface area. Therefore, in the present study, Sal flower has been chosen to synthesize the activated carbon for supercapacitor application. The waste precursor

Received 16 November 2021, received in revised form 3 December 2021, accepted 3 January 2022

*Surface Engineering & Tribology Division, Council of Scientific and Industrial Research-Central Mechanical Engineering Research Institute, Durgapur 713209, India

**Academy of Scientific and Innovative Research (AcSIR), CSIR-CMERI, Campus, Durgapur 713209, India

***Department of Nano Convergence Engineering, Jeonbuk National University, Jeonju 54896, Korea

†Corresponding authors, Prof. Nam Hoon Kim (E-mail: nhk@jbnu.ac.kr) & Dr. Tapas (E-mail: tkuila@gmail.com)

materials are usually activated through physical process or using chemical activating agents like H_3PO_4 , KOH or ZnCl_2 [7]. The chemical activator is able to tune the morphology and also to functionalize the surface of the activated carbon, which improves the electrochemical performance of the supercapacitor. Although, lots of works have been performed to use different chemical activators, such as KOH, ZnCl_2 , NaOH, H_3PO_4 , etc., to synthesize activated carbon from various waste materials, but the effect of various activators on activated carbon from certain wastes is not reported [8]. Therefore, this study focuses on the activated carbon derived from the Sal (*Shorea robusta*) flower using three different chemical activating agents H_3PO_4 , KOH or ZnCl_2 and investigated its utility as supercapacitor electrode. The obtained activated carbon delivered high specific capacitance and good cyclic stability in aqueous electrolyte. It shows that the derived activated carbon was graphitic in nature and the disorder of the graphitic carbon changed with the chemical activating agents.

2. MATERIALS AND EXPERIMENTAL

2.1 Materials

The flowers of Sal (*Shorearobusta*) were collected from the campus of CSIR-CMERI Durgapur, India. Potassium hydroxide (KOH), phosphoric acid (H_3PO_4), zinc chloride (ZnCl_2), hydrochloric acid (HCl) and N,N-dimethyl formamide (DMF) were purchased from the Merck specialties private Limited (Mumbai, India). Absolute ethanol with ~99.9% purity was procured from Hi-Media Laboratories Pvt. Ltd., Mumbai, India. Polyvinylidene fluoride (PVDF) was obtained from Akzo Nobel Amides Co., Ltd. (Kyungpuk, South Korea). Nickel foam (NF) was obtained from Shanghai Winfay New Material Co., Ltd., China.

2.2 Preparation of composite materials

The activated carbon was synthesized from the flower of *Shorea robusta* in a two-step process. At first, the flowers were repeatedly washed with tap water and then with de-ionised (DI) water to remove the dust impurities, dried in open air under the Sun followed by oven drying at 120°C for 12 h to reduce the moisture content. The resulting samples were grinded into powder and pre-carbonized by heating at 200°C for ~3 h under vacuum condition and cooled to room temperature. For chemical activation, ~2 g of pre-carbonized sample was added into the 20 ml of 3 M ($M = \text{Molarity}$) aqueous KOH solution followed by continuous stirring for 12 h at 400 rpm. Samples were collected by filtration and washing for several times with DI water-ethanol (1:1) mixture and dried inside a vacuum oven for 12 h at 80°C . The oven dried samples were carbonised inside a tube furnace at 700°C for 2 h under the continuous flow of N_2 gas. The obtained

product was collected after cooling the furnace and washed repeatedly with HCl and water-ethanol mixture (1:1) followed by drying inside a vacuum oven at 60°C for 12 h. The final product was designated as ACSF-K. The products ACSF-Z and ACSF-H were obtained by using 20 ml 3 M aqueous solution of ZnCl_2 and 20 ml 85% H_3PO_4 aqueous solution (3 M), respectively as the activating agents while keeping the other experimental conditions identical. On the basis of chemical activating agents such as KOH, ZnCl_2 and H_3PO_4 the obtained final products were designated as ACSF-K, ACSF-Z and ACSF-H, respectively. In order to compare the effect of the concentration of activated agents, another two activated carbon samples were prepared using 1 M (ACSF-K1) and 5 M KOH (ACSF-K2) solutions.

2.3 Characterization

The chemical composition and crystal structure of the synthesized electrode materials were carried out with powder x-ray diffractometer (PXRD), Rigaku X-ray powder diffractometer via Cu K α radiation. To observe the morphologies of the samples, Field-emission scanning electron microscopy (FE-SEM) was recorded using the instrument Sigma HD, Carl Zeiss, Germany. Fourier transforms infrared (FT-IR) spectrometer (Perkin Elmer RXI) was used to detect the presence of functional groups using KBr pellets in the range of 400-4000 cm^{-1} . Witec alpha 300 R with a laser wavelength of 532 nm was used to record the Raman spectra of the developed electrode materials.

2.4 Electrochemical characterization

The electrochemical properties of the synthesized electrodes materials were evaluated in three-electrode setup with PARSTAT 3000 workstation (Princeton Applied Research, USA). In three-electrode setup, active slurry mixture deposited on nickel foam (NF), Ag/AgCl with saturated KCl, Pt wire and 6 M KOH were used as working electrode, reference electrode, counter electrode and electrolyte, respectively. The active slurry was prepared by mixing the active materials, PVDF as binder (90:10) in 10 ml DMF solvent and mixed slurry drop cast on NF current collector. Before using as current collector, NF was treated with 5% HCl and DI water under ultrasonication followed by washing several times to remove the surface impurities and dried inside the vacuum oven.

The specific capacitance (SC) of the electrodes was measure by using following equation:

$$\text{SC} = i \times \Delta t / m \times \Delta V \quad (1)$$

Here, 'i' refer to the applied current, ' Δt ' is the total discharge time of GCD, 'm' is the weight of active electrode materials and ' ΔV ' represent the working potential window.

3. RESULTS AND DISCUSSIONS

3.1 Physicochemical characterizations analysis

Fig. 1a demonstrate a sharp peak at $2\theta \approx 25^\circ$ region in ACSF-K and ACSF-Z samples corresponds to 002 plane of graphitic carbon. However, for ACSF-H, this peak shifted to $2\theta \approx 26.6^\circ$ and the reduced peak intensity indicated its amorphous nature compared to the others two. Another small intense peak at $2\theta \approx 43.5^\circ$ is generated in all the materials due to the 101 plane of graphitic carbon, which signified the amorphous nature of the samples. A small peak at $2\theta \approx 28^\circ$ corresponding to the 111 plane of graphitic carbon was observed in ACSF-K and ACSF-Z electrodes suggesting the polycrystalline nature of the derived carbon. This peak also indicates that the structure of graphitic carbon is more disordered due to the presence of Zn and K used during the activation process. However, the absence of peak at $2\theta \approx 28^\circ$ in ACSF-H sample indicated low disordered structure of synthesizes graphitic carbon [9]. Therefore, the PXRD analysis clearly shows the formation of amorphous graphitic carbon in all the samples and the graphitic character is reduced from the ACSF-K to ACSF-Z and ACSF-H electrode materials [9,10].

The degree of disorder and chemical structure of the synthesized electrode materials were examine by Raman spectroscopy as shown in Fig. 1b. Raman spectroscopy is considered as the sensitive technique used to find out the

disorder in sp^2 carbon material. The Raman spectrum demonstrated two sharp peaks at ~ 1345 and 1580 cm^{-1} region related to the D and G bands [3,4]. The D band is originated due to the disorder in the graphite carbon corresponding to the A_{1g} symmetry. This peak indicated the presence of amorphous regions in the graphitic carbon. G-Peak corresponds to the E_{2g} vibration of phonon at the Brillouin zone centre is attributed to the in-plane stretching motion of sp^2 carbon atom [13]. The observed sharp D and G bands were another conformation for the formation of graphitic carbon. Raman spectroscopy showed the increase of D band intensity in the order of ACSF-Z < ACSF-H < ACSF-K compared to the G band. The quality of the samples was determined by calculating the ratio of D and G bands. The Raman spectrum demonstrates the I_D/I_G ratio of ACSF-K (1.2) is higher compared to the ACSF-Z (0.62) and ACSF-H (0.74), indicating that the presence of disordered carbon in ACSF-K was higher than the others. The disordered structure enhanced the reactive sites of carbon, which is beneficial for ion storage capability of the samples. Another peak generated at $\sim 2700\text{ cm}^{-1}$ region in all the samples, referred to the 2D band, which indicated the formation of layered graphitic carbon [4,13]. The number of layers in the graphitic carbons can be possibly determined from the intensity of the 2D band. The sharp 2D bands of ACSF-H compared to ACSF-K and ACSF-Z suggested the lower number of graphitic carbon in ACSF-Z electrode [11,12].

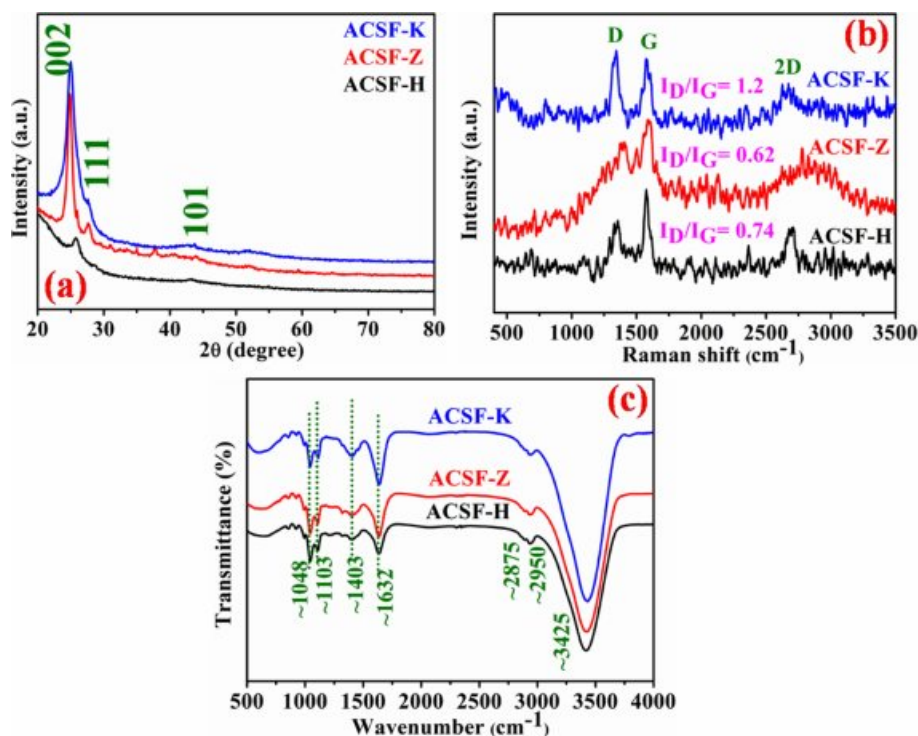


Fig. 1. (a) PXRD pattern of all the synthesized materials (b) Raman spectra and (c) FT-IR spectra of synthesized electrode materials, respectively

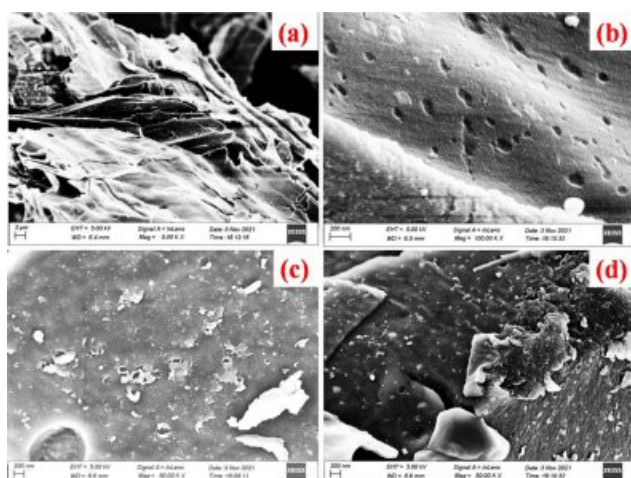


Fig. 2. (a,b) FE-SEM images of ACSF-K electrode material, (c,d) FE-SEM images of ACSF-Z and ACSF-H electrode material, respectively

The surface properties and the presence of heteroatom on the synthesized graphitic carbons were analyzed with FT-IR spectroscopy. The FT-IR spectra of ACSF-K, ACSF-Z and ACSF-H are shown in Fig. 1c. A broad transmittance band observed at $\sim 3425\text{ cm}^{-1}$ due to the stretching mode of hydroxyl groups (O-H) and absorbed water molecules [13]. Two weak transmittance peaks also observed in all the three samples at ~ 2950 and 2875 cm^{-1} associated with the asymmetric and symmetric stretching vibration of $-\text{CH}_2-$ groups, respectively [13,14]. A sharp intense peak at 1632 cm^{-1} is

attributed to the $-\text{C}=\text{O}$ stretching oscillations of carboxylic and ketone functional groups. Another peak observed at 1403 , 1103 and 1048 cm^{-1} represents the bending vibration of C-H bond, symmetric C-C and C-O stretching mode, respectively. FT-IR spectra also illustrated that the peak intensities at 1632 and 1403 cm^{-1} for ACSF-K were higher compared to the other two electrode materials, suggesting that the carbon was more oxygenated and well graphitized in ACSF-K electrode [13,14].

The surface morphology of the ACSF-K samples was analyzed from the FE-SEM images. Fig. 2a confirms the formation of graphitic layered structure. Fig. 2b illustrates the large number of small holes and cracks on the surface of the graphitic carbon during annealing which increased the effective active sites for diffusion of electrolyte and delivered higher specific capacitance of the electrode materials. The FE-SEM images of ACSF-Z (Fig. 2c) and ACSF-H (Fig. 2d) electrodes also showed the formation of graphitic type layered structure [15,16].

3.2 Electrochemical properties

The electrochemical properties of the synthesized ACSF-K, ACSF-Z and ACSF-H electrode materials were investigated in three-electrode configuration using 6 M KOH as electrolyte. Cyclic voltammetry (CV), galvanostatic charge-discharge (GCD) and electrochemical impedance spectroscopy (EIS) were carried out to analyze the electrochemical properties of the developed electrode materials. Fig. 3a shows the comparable CV curves of all three electrode materials at a scan rate of 30 mV s^{-1} in the range of 0 to 0.4 V working potential. All the

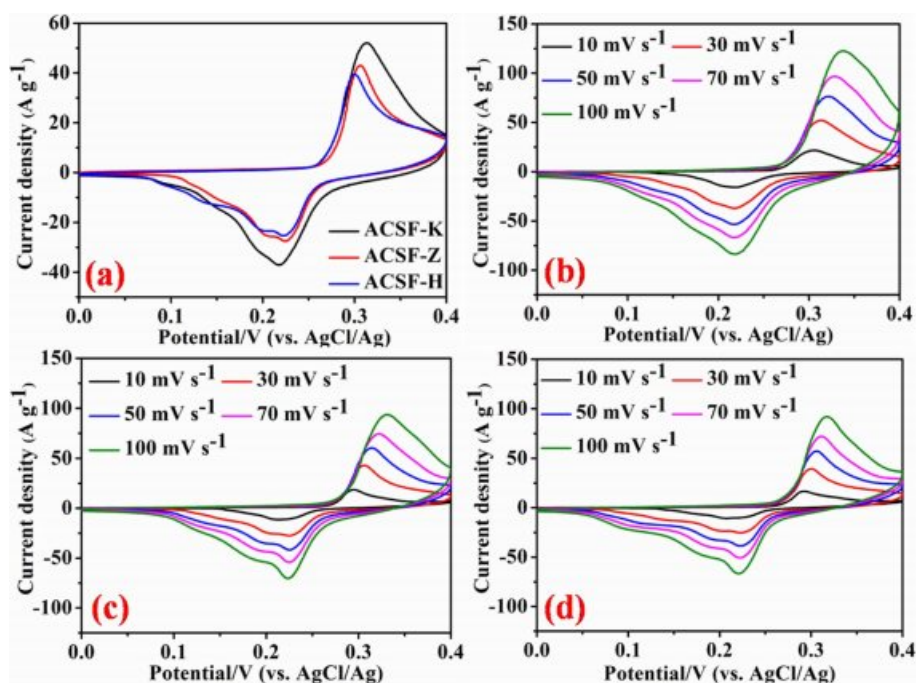


Fig. 3. (a) Comparable CV curves (b-d) CV curves at variable scan rates of 10 - 100 mV s^{-1} of ACSF-K, ACSF-Z and ACSF-H electrodes, respectively.

electrode demonstrated a pair of broad redox peaks, indicating the electron transfer faradic reaction is happening during the charge storage process [1,2,4]. It is found that the ACSF-K electrode covered larger CV curve area compared to ACSF-Z and ACSF-H electrode implying the higher energy storage capability of ACSF-K electrode. Further CV curves of the ACSF-K (Fig. 3b), ACSF-Z (Fig. 3c) and ACSF-H (Fig. 3d) electrodes were analyzed at variable scan rates from 10 to 100 mV s^{-1} . It was found that with increasing the scan rates, redox peak current increases and peak position was slightly shifted towards positive and negative potential areas, suggesting the good rate capability and faster charge transfer properties of the electrodes [1,2,8].

The specific capacitances of all the synthesized electrodes were calculated from the discharging time of the respective GCD curves using equation (1). Fig. 4a demonstrate the GCD curves of the synthesized three electrode materials at 2 A g^{-1} constant current density and showed that the specific capacitance of ACSF-K (610 F g^{-1}) was higher compared to the ACSF-Z (560 F g^{-1}) and ACSF-H (470 F g^{-1}) electrodes. The GCD curves of all the electrodes showed a clear voltage plateau in both of charge and discharge process, signifying the faradic charge storage process. The higher capacitance of ACSF-K electrodes mainly attributed to the presence of highly disorder graphitic carbons, facilitated large number of electrochemical reactive sites [2,3]. Rate capability is an important characteristic of any supercapacitor electrode materials. To measure the specific capacitance of the ACSF-K (Fig. 4b), ACSF-Z (Fig. 4c) and ACSF-H (Fig. 4d) electrodes, the GCD was performed at 2-10 A g^{-1} variable current density. In order to investigate the effect of concentration of activating agent (KOH) on the electrochemical performance of the ACSF-K electrodes, the CV (Fig. 4e) and GCD (Fig. 4f) was carried out.

The CV and GCD curves showed that the ACSF-K1 and ACSF-K2 electrodes had lower curves area and discharge time compared to the ACSF-K electrode. This observation suggested that all the pre-carbonized materials were not activated equally at lower concentration (1M) and higher concentration (5M) possibly decreased the electrochemical active sites by deteriorating the ion diffusion/adsorption processes [17]. Therefore, concentration of the activating agent is a crucial factor in controlling the supercapacitor performance of the derived activated carbon.

Fig. 5a shows the higher rate capability of ACSF-K (~88%) compared to ACSF-Z (~76%) and ACSF-H (~72%), when current density increased from 2-10 A g^{-1} . The higher rate capability of the ACSF-K and ACSF-Z electrodes is attributed to the highly disordered graphitic carbons [2-4], which served as the electrolyte reservoirs and enabled a rapid and short ion diffusion path [14,15].

The interfacial electrochemical charge transfer kinetics of the electrodes was investigated from the EIS. The EIS was measured with 10 mV open circuit potential in the 0.1 to 10000 Hz frequency range. A straight line at low frequency and a semi circle at high frequency regions were observed in the Nyquist plot as shown in Fig. 5b. The straight line related to the diffusion of the electrolyte from the electrode surface is known as Warburg resistance (W_o). The semi circle at higher frequency region correlated to the transfer of charge in the electrode material is known as charge transfer (R_{ct}) resistance. To acquire the EIS data, using Z-View software obtained Nyquist plots were fitted with the help of Randles circuit model (inset of Fig. 5b) and the acquired data (Fig. 5c-e) are summarized in Table 1. The fitted curves of the Nyquist plots demonstrated four parts of uncompensated resistance (R_s), constant phase element (CPE), Charge transfer resistance (R_{ct})

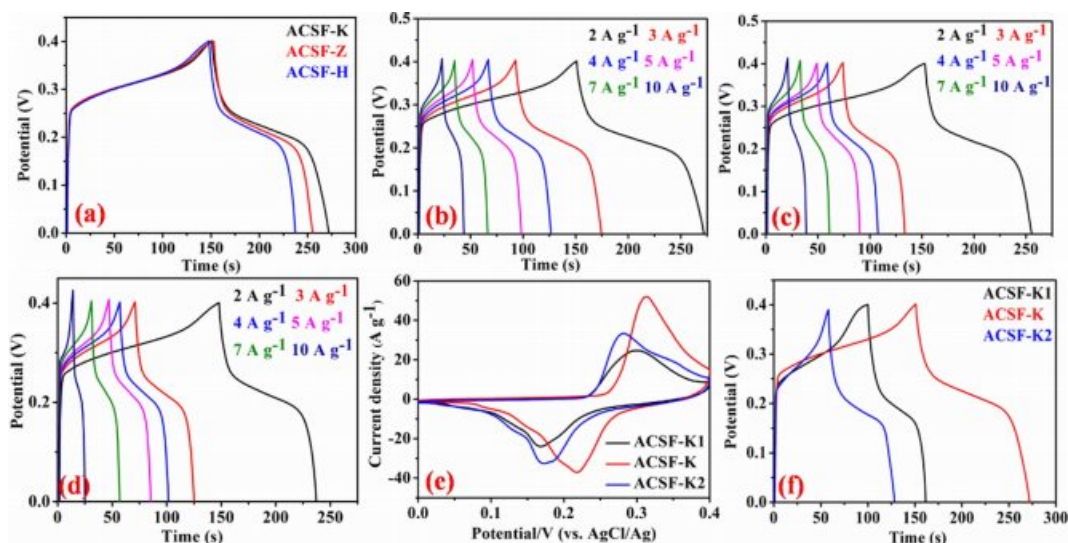


Fig. 4. (a) Comparable GCD curves (b-d) GCD curves of ACSF-K, ACSF-Z and ACSF-H electrodes, respectively at different current density of 2-10 A g^{-1} (e,f) Comparable CV and GCD curves of the electrodes at different concentration of KOH

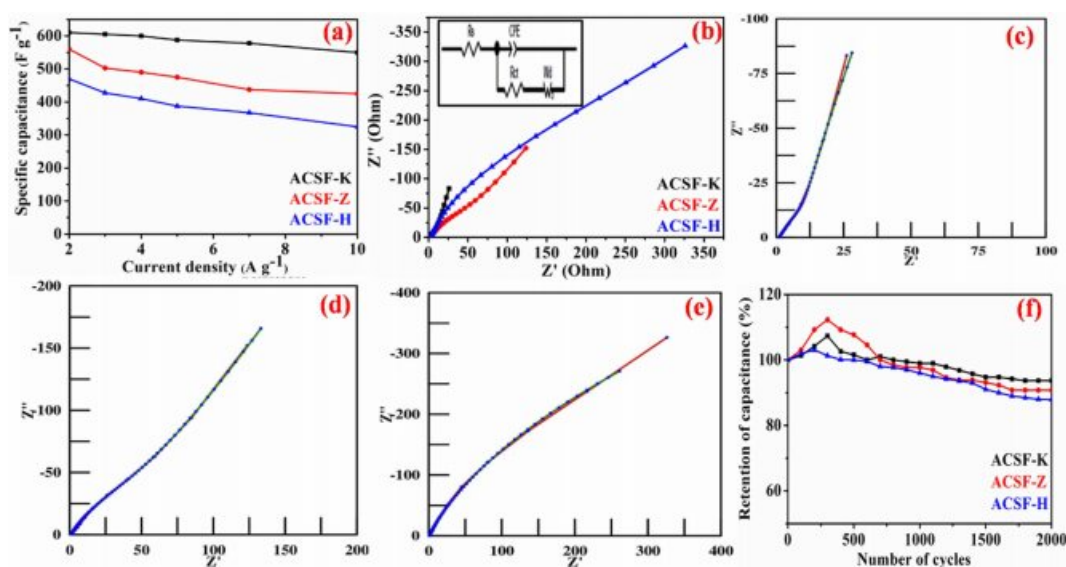


Fig. 5. (a) variation of specific capacitance with current density of ACSF-K, ACSF-Z and ACSF-H electrodes (b) EIS spectra of the electrodes (inset figure; Randle circuit model) (c-e) Z-view fitted EIS spectra of ACSF-K, ACSF-Z and ACSF-H electrode, respectively (f) measurement of cyclic stability of the three electrodes up to 2000 GCD cycles

Table 1. Z-view fitted values of electrodes corresponded to Fig. 5(c-e)

Electrodes	R_s (Ω)	CPE-T	CPE-P	R_{ct} (Ω)	W-R	W-T	W-P
ACSF-K	1.1	0.011	0.75	8	100	0.58	0.5
ACSF-Z	1	0.0025	0.73	35	150	0.65	0.32
ACSF-H	0.8	0.0022	0.77	46	450	0.85	0.15

and Warburg (W_0) resistance. R_s stand for the contact resistance of the electrode materials with the electrolyte and current collector. The CPE values represented the deviation of ideal capacitive behavior of the electrode and it was divided in capacitance range (CPE-T) and phase angle parameters (CPE-P) [2,3]. The lower R_{ct} value of ACSF-K (8 Ω) compared to ACSF-Z (35 Ω) and ACSF-H (46 Ω) electrodes implied the good charge transfer kinetics and higher electrical conductivity of the ACSF-K electrode [10-12]. It is due to the formation of highly disorder graphitic carbons of ACSF-K electrode, which were in agreement with the better capacitance performance of the electrode. The lower Warburg resistance value (100 Ω) of ACSF-K also suggested the shorter ion diffusion path and faster rate of ion diffusion compared to ACSF-Z (150 Ω) and ACSF-H (450 Ω) [2-4].

The cycling performance is another important property of supercapacitor. The cyclic performance of the synthesized electrodes was investigated by continuous GCD cycles at 10 A g^{-1} constant current density and shown in Fig. 5f. Cyclic performance exhibited that after continuous 2000 GCD cycles the ACSF-K retained ~94% of its initial capacitance, which is better compared to ACSF-Z (91.7%) and ACSF-H (~88%) electrodes, respectively. Fig. 4f also showed after few cycles to ~500 cycles the capacitance increased much more for all the

electrodes, which may due to the perfectly witting and activation of the materials [1-3].

4. CONCLUSIONS

The flower of *Shorea robusta*, a bio-waste was successfully used as the raw materials for the synthesis of activated carbons for application as supercapacitor electrode material. The activated carbons synthesize through chemical activation process using KOH, $ZnCl_2$ and H_3PO_4 activating agents. The physicochemical analyses demonstrated that the obtained activated carbons were graphitic in nature and the degree of disorder of the graphitic carbons was dependent on the activating agents. The formation of disorder graphitic carbons and presence of functional groups on the carbons opens up larger electroactive sites and well electrode to electrolyte interaction. The ACSF-K electrode showed a capacitance value of 610 F g^{-1} at a current density of 2 A g^{-1} , which is higher than ACSF-Z (560 F g^{-1}) and ACSF-H (470 F g^{-1}) Electrode material under the identical current density. The synthesized graphitic carbons also demonstrated good rate capability and higher stability as supercapacitor electrodes. All the physicochemical and electrochemical characterizations illustrated that the flower of *Shorea robusta* derived activated carbon is a good choice for

supercapacitor electrode material.

ACKNOWLEDGEMENT

Authors are thankful to JCBCAT, Kolkata, DRDO, Ministry of Defence, Government of India for the financial support [DFTM/02/3111/M/01/JCBCAT/1288/D(R&D), Dated: 07/07/2017]. Authors are also thankful to the Director of CSIR-CMERI, Durgapur.

REFERENCES

1. Wang, L., Shu, T., Guo, S., Lu, Y., Li, M., and Nzabahimana, J., H., "Fabricating Strongly Coupled V_2O_5 @PEDOT Nanobelts/Graphene Hybrid Films with High Areal Capacitance and Facile Transferability for Transparent Solid-State Supercapacitors", *Energy Storage Materials*, Vol. 27, 2020, pp. 150-158.
2. Jana, M., Samanta, P., Murmu, N.C., Kim, N.H., Kuila, T., and Lee J.H., "Development of Cobalt Sulfide-graphene Composite for Supercapacitor Applications", *Composites Research*, Vol. 29, No. 4, 2016, pp. 167-172.
3. Ghosh, S., Samanta, P., Murmu, N.C., and Kuila, T., "Investigation of Electrochemical Charge Storage in Nickel-cobalt selenide/reduced Graphene Oxide Composite Electrode and Its Hybrid Supercapacitor Device", *Journal of Alloys and Compounds*, Vol. 835, 2020, pp. 155432.
4. Ghosh, S., Samanta, P., Murmu, N.C., and Kuila, T., "Enhancement of the Electrochemical Performance of a Novel Binder-Free Ni_3S_2 @ Co_3S_4 / Mn_3O_4 -RGO Heterostructure through Crystallinity and Band Gap Modification for Flexible Supercapacitors", *Energy Fuels*, Vol. 35, 2021, pp. 13389-13401.
5. Rufford, T.E., Hulicova-Jurcakova, D., Khosla, K., Zhu, Z., and Lu, G.Q., "Microstructure and Electrochemical Double-layer Capacitance of Carbon Electrodes Prepared by Zinc Chloride Activation of Sugar Cane Bagasse", *Journal of Power Sources*, Vol. 195, 2010, pp. 912-918.
6. Gupta, S.K., Ranjan, R., Singh, M., and Verma, D.S., "Pharmacognostical and Phytochemical Study of Sala (Shorea robusta)", *Journal of Medical Science and Clinical Research*, 2017, Vol. 05, pp. 28021-28029.
7. Wu, M., Li, P., Li, Y., Liu, J., and Wang, Y., "Enteromorpha Based Porous Carbons Activated by Zinc Chloride for Supercapacitors with High Capacity Retention", *RSC Advances*, Vol. 5, 2015, pp. 16575-16581.
8. Bagheri, N., and Abedi, J., "Preparation of High Surface Area Activated Carbon from Corn by Chemical Activation Using Potassium Hydroxide", *Chemical Engineering Research and Design*, Vol. 87, 2009, pp. 1059-1064.
9. Sarkar, S., Arya, A., Gaur, U.K., and Gaur, A., "Investigations on Porous Carbon Derived from Sugarcane Bagasse as an Electrode Material for Supercapacitors", *Biomass and Bioenergy*, Vol. 142, 2020, pp. 105730.
10. Rawala, S., Joshia, B., and Kumar, Y., "Synthesis and Characterization of Activated Carbon from the Biomass of Saccharum Bengalense for Electrochemical Supercapacitors", *Journal of Energy Storage*, Vol. 20, 2018, pp. 418-426.
11. Ghosh, S., Samanta, P., Samanta, P., Murmu, N.C., and Kuila, T., "Investigation of Electrochemical Charge Storage Efficiency of $NiCo_2Se_4$ /RGO Composites Derived at Varied Duration and Its asymmetric Supercapacitor Device", *Energy Fuels*, Vol. 34, 2020, pp. 13056-13066.
12. Hu, S.C., Cheng, J., Wang, W.P., Sun, G.T., Hu, L.L., Zhu, M.Q., and Huang, X.H., "Structural Changes and Electrochemical Properties of Lacquer Wood Activated Carbon Prepared by Phosphoric Acid-chemical Activation for Supercapacitor Applications", *Renewable Energy*, Vol. 177, 2021, pp. 82-94.
13. Sivachidambaram, M., Judith Vijaya, J., John Kennedy, L., Jothiramalingam, R., Al-Lohedan, H.A., Munusamy, M.A., Elanthamilane E., and Princy Merline, J., "Preparation and Characterization of Activated Carbon Derived from the Borasus Flabellifer Flower as an Electrode Material for Supercapacitor Applications", *New Journal of Chemistry*, Vol. 41, 2017, pp. 3939-3949.
14. Liu, Q.S., Zheng, T., Wang, P., and Guo, L., "Preparation and Characterization of Activated Carbon from Bamboo by Microwave-induced Phosphoric Acid Activation", *Industrial Crops and Products*, Vol. 31, 2010, pp. 233-238.
15. Guo, Y., Tan, C., Sun, J., Li, W., Zhang, J., and Zhao, C., "Porous Activated Carbons Derived from Waste Sugarcane Bagasse for CO_2 Adsorption", *Chemical Engineering Journal*, Vol. 381, 2020, 122736.
16. Chen, H., Yu, F., Wang, G., Chen, L., Dai, B., and Peng, S., "Nitrogen and Sulfur Self-Doped Activated Carbon Directly Derived from Elm Flower for High-Performance Supercapacitors", *ACS Omega*, Vol. 3, 2018, pp. 4724-4732.
17. Sahoo, M.K., and Rao, G.R., "A High Energy Flexible Symmetric Supercapacitor Fabricated Using N-doped Activated Carbon Derived from Palm Flowers", *Nanoscale Adv.*, Vol. 3, 2021, pp. 5417-5429.